Detection of Nickel in Fish Organs with a Two-Photon Fluorescent Probe

ARTICLE *in* CHEMISTRY - A EUROPEAN JOURNAL · FEBRUARY 2012

Impact Factor: 5.73 · DOI: 10.1002/chem.201103191 · Source: PubMed

7 AUTHORS, INCLUDING:

Lim Chang Su
Korea University
46 PUBLICATIONS **1,363** CITATIONS
SEE PROFILE

Hyun SOO Kim
Dong-A University
374 PUBLICATIONS **4,227** CITATIONS
SEE PROFILE

Ohyun Kwon
Samsung Advanced Institute of Technology
66 PUBLICATIONS **1,922** CITATIONS
SEE PROFILE

DOI: 10.1002/chem.201103191

Detection of Nickel in Fish Organs with a Two-Photon Fluorescent Probe

Min Young Kang,[a] Chang Su Lim,[a] Hyun Soo Kim,[a] Eun Won Seo,[b] Hwan Myung Kim,*[b] Ohyun Kwon,*[c] and Bong Rae Cho*[a]

Abstract: Molecular imaging by two-photon microscopy (TPM) has become indispensable to the study of biology/medicine owing to its capability of imaging deep inside intact tissues. To make TPM a more-versatile tool, a large variety of two-photon probes are needed. Herein, we report a new two-photon fluorescent probe (ANi2) that can be excited by 750 nm femtosecond pulses and detect Ni^{2+} ions in fresh fish organs at 90–175 μm depth without interference from the pH value or from other biologically relevant species through the use of TPM. TPM images of fish organs labeled with ANi2 revealed that Ni^{2+} ions accumulate in fish organs in the order: kidney > heart > gill ≥ liver. Moreover, a linear relationship was found between the two-photon-excited fluorescence (TPEF) and the inductively coupled plasma mass spectrometry intensities (ICP-MS), thereby allowing the quantitative measurement of Ni^{2+} ions in live tissue.

Keywords: fish · fluorescent probes · live tissue · nickel · two-photon microscopy

Introduction

Nickel is used in many industrial and consumer products, including stainless steel, magnets, coinage, rechargeable batteries, and special alloys. Nickel enters the environment via both natural and human activities. The toxicity of nickel is low but excess nickel accumulation can cause lethal effects in aquatic ecosystems.[1] The fish living in the polluted water can take in Ni^{2+} ions through their mouth and through their skin, which can then be accumulated in different organs.[2a] The average intake of nickel by humans ranges from 300–600 $\mu g\,day^{-1}$.[2b,c]

To prevent nickel-related problems, it is important to detect trace amounts of Ni^{2+} ions in the early stage of contamination. The standard techniques for measuring total nickel amounts are atomic absorption and inductively coupled plasma mass spectrometry (ICP-MS). Fluorescence measurement using Ni^{2+}-selective fluorescent probes can be a compliment to these methods. To date, only a few small-molecule fluorescent probes for Ni^{2+} ions have been reported;[3,4] they are derived from anthracene, $[Ru(bipy)_3]$ (bipy = 2,2′-bipyridine), fluorene, and BODIPY (boron-dipyrromethene) as the fluorophores, and dioxotetramine and *N,N*-bis[2-(carboxylmethyl)thioethyl]amine (CTEA) as the receptors. Among these probes, BODIPY-derived NS1 has been utilized to detect intracellular Ni^{2+}-ion levels by confocal microscopy.[5] This small molecule (< 1 kD) does not require transfection like its protein counterparts.[6–8] However, the use of these probes in one-photon microscopic analysis requires short excitation wavelengths (< 500 nm), which limits their use in tissue imaging owing to their shallow penetration depth (< 80 μm). To detect Ni^{2+} ions deep inside the fish organs, the use of two-photon microscopy (TPM) is crucial. TPM, which utilizes two photons of lower energy for the excitation step, has the advantages of increased penetration depth (> 500 μm), localized excitation, and prolonged observation time, thereby allowing deep-tissue imaging.[9–11] However, there have been no reported TP probes for Ni^{2+} ions.

To develop an efficient TP probe for Ni^{2+} ions, we linked the Ni^{2+} receptor, CTEA, to the reporter 2-acetyl-6-dialkylaminonaphthalene (acedan) through spacer groups according to the following requirements of the probe: 1) an appreciable water solubility to stain the cells and tissues, 2) high selectivity for Ni^{2+} ions, 3) significant TP cross-section for a bright TPM image, 4) pH resistance, and 5) high photostability (ANi1 and ANi2; Scheme 1). We chose acedan as the fluorophore because TP probes derived from acedan have been successfully utilized in live-tissue imaging,[12–14] and we chose CTEA as the receptor because it had previously been used for the detection of Ni^{2+} ions by Chang and co-workers.[5] Herein, we report the design, synthesis, spectroscopic

[a] M. Y. Kang,[+] C. S. Lim,[+] H. S. Kim, Prof. Dr. B. R. Cho
Department of Chemistry, Korea University, 145, Anam-ro, Sungbuk-gu, Seoul, 136-713 (Korea)
Fax: (+82) 2-3290-3544
E-mail: chobr@korea.ac.kr

[b] E. W. Seo, Prof. Dr. H. M. Kim
Division of Energy Systems Research, Ajou University
Suwon, 443-749 (Korea)
Fax: (+82) 31-219-1615
E-mail: kimhm@ajou.ac.kr

[c] Dr. O. Kwon
Samsung Advanced Institute of Technology
Suwon (Korea)
Fax: (+82) 32-3210-3222
E-mail: tigertom@dreamwiz.com

[+] These two authors contributed equally to this work.

Supporting information for this article is available on the WWW under http://dx.doi.org/10.1002/chem.201103191.

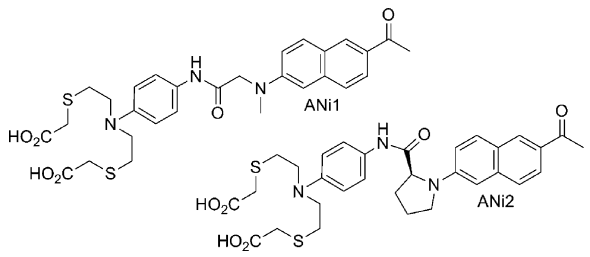

Scheme 1. Structures of probes ANi1 and ANi2.

analysis (in both one- and two-photon mode), and TPM imaging applications of ANi2.

Results and Discussion

Design and photophysical properties of ANi1 and ANi2: It has been well-established that the combination of acedan as the reporter with a specific receptor through a glycinamide linkage is a simple and effective strategy to design a turn-on TP probe.[12–14] We have designed two probes, ANi1 and ANi2, using glycinamide and prolinamide as the linkers, respectively (Scheme 1). The Ni^{2+} receptor (**3**) was prepared by the reaction between compound **1** and methyl thioglycolate followed by reduction. Coupling between compounds **A** and **3**, followed by hydrolysis produced ANi1 in 33% yield. ANi2 was produced according to the same procedure, by using compound **B** in the place of compound **A** (Scheme 2).

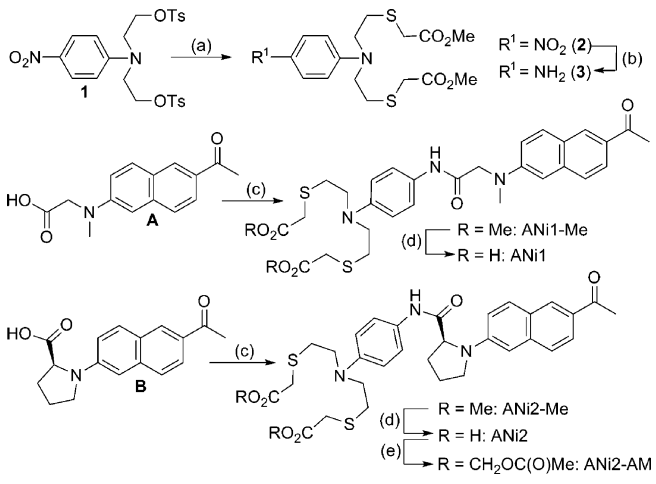

Scheme 2. Synthesis of probes ANi1, ANi2, and ANi2-AM. Reaction conditions: a) methyl thioglycolate, Cs_2CO_3, DMF; b) $SnCl_2$, MeCN/EtOH; c) DCC, HOBt, compound **3**, CH_2Cl_2; d) KOH, EtOH, EtOAc; e) $BrCH_2OC(O)CH_3$, DIPEA, DMF. DCC = *N*,*N*′-dicyclohexylcarbodiimide, HOBt = 1-hydroxybenzotriazole, DIPEA = *N*,*N*-diisopropylethylamine.

The solubilities of ANi1, ANi2, and ANi2-AM in HEPES buffer ([HEPES] = 20 mM, pH 7.1), as determined by the fluorescence method,[12,13] were in the range 2.1–9.0 μM (see the Supporting Information, Figure S1); these values are sufficient to stain the cells. In HEPES buffer, ANi1 and ANi2 showed absorption maxima at 365 nm ($\varepsilon = 13\,500$) and 375 nm ($\varepsilon = 17\,900$) and fluorescence maxima at 500 nm ($\Phi = 0.017$) and 500 nm ($\Phi = 0.0080$), respectively (Table 1). The absorption and emission spectra of ANi1 and ANi2 showed gradual red shifts with increasing solvent polarity, in the order: 1,4-dioxane < DMF < EtOH < HEPES buffer. The large solvatochromic shifts observed with increasing solvent polarity indicate the utility of ANi1 and ANi2 as environment-sensitive probes (see the Supporting Information, Figure S2 and Table S1).

Table 1. Photophysical properties of ANi1 and ANi2 in buffer.[a]

Compound	$\lambda_{max}^{(1)}$ ($10^{-4}\varepsilon$) [nm][b]	λ_{max}^{fl} [nm][c]	Φ[d]	K_d^{OP}/K_d^{TP} [μM][e]	*FEF*[f]	$\lambda_{max}^{(2)}$ [nm][g]	Φ[h]
ANi1	365 (1.35)	500	0.017	–	–	–	–
ANi1+Ni^{2+}	365	500	0.088	100/100	5.0	750	32
ANi2	375 (1.79)	500	0.0080	–	–	–	–
ANi2+Ni^{2+}	375	500	0.21	88/89	26	750	90

[a] All data were measured in HEPES buffer (20 mM HEPES, pH 7.1) in the absence and presence of free Ni^{2+} ions (1 mM) unless otherwise noted. [b] λ_{max} of the one-photon-absorption spectra; the numbers in parentheses are molar extinction coefficients in $M^{-1}cm^{-1}$. [c] λ_{max} of the one-photon-emission spectra. [d] Fluorescence quantum yield, (±15)%. [e] Dissociation constants for Ni^{2+} ions measured by one-proton (K_d^{OP}) and two-photon processes (K_d^{TP}), (±8)%. [f] Fluorescence-enhancement factor, $(F-F_{min})/F_{min}$. [g] λ_{max} of the two-photon-excitation spectra. [h] Two-photon action cross-section in 10^{-50} cm^4 s photon^{-1} (GM).

When Ni^{2+} ions were added to ANi1 in HEPES buffer, the fluorescence intensity increased gradually without affecting the absorption spectrum, presumably because of the blocking of photoinduced electron-transfer (PeT) by the complexation with the metal ion (Figure 1; also see the Supporting Information, S3). The fluorescence enhancement factors [$FEF = (F-F_{min})/F_{min}$] for the one- and two-photon (TP) processes were both 5.0. Probe ANi2 showed similar behavior, except that the *FEF* (26) was much larger, presumably as a result of the lower fluorescence quantum yield ($\Phi = 0.017$ versus 0.0080) in the absence of Ni^{2+} ions, and higher fluorescence quantum yields ($\Phi = 0.088$ versus 0.21) in the presence of excess Ni^{2+} ions than those for ANi1 (Table 1). DFT (density functional theory) calculations at the B3LYP/6-31G** level revealed that the highest molecular orbital energies of CTEA, ANi1, and ANi2 were −4.351, −4.785, and −4.938 eV, respectively (see the Supporting Information, Table S2 and Figure S4).[15,16] Hence, the PeT from CTEA to ANi2 might occur more efficiently on thermodynamic grounds, thereby decreasing the fluorescence quantum yield.[15,16] On the other hand, the larger fluorescence quantum yield for ANi2-Ni^{2+} complex can be attributed to the prolinamide ring, which may have reduced the vibrational relaxation pathways compared to the open-chain analogue (ANi1). This result underlines the advantage of introducing prolinamide as the donor in the design of turn-on probes.

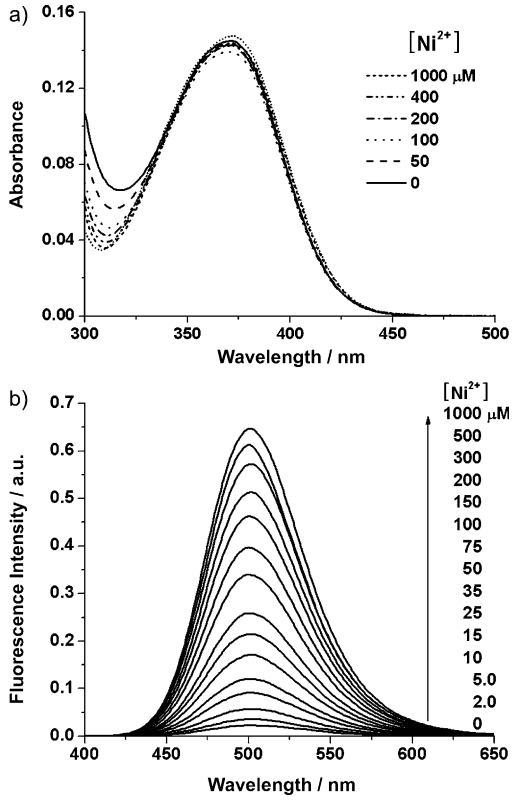

Figure 1. One-photon absorption (a) and emission (b) spectra of probe ANi2 (2 μM) in the presence of free Ni^{2+} ions (0–1.0 mM); these data were obtained in HEPES buffer. The excitation wavelength was 375 nm.

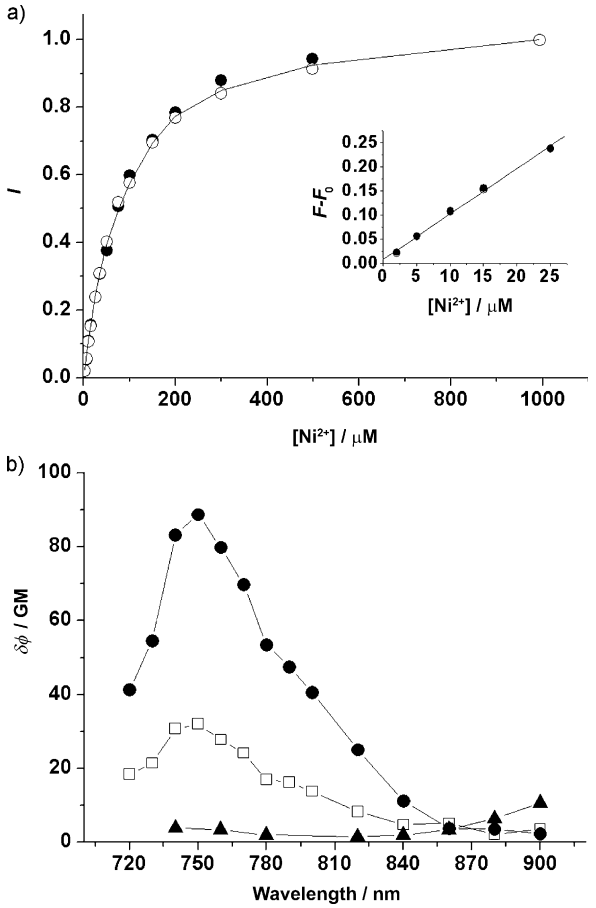

Figure 2. a) One-photon (●) and two-photon fluorescence titration curves (○) for the complexation of ANi2 (2 μM) with Ni^{2+} ions (0–1 mM; calculated values are represented by ——). b) Two-photon action spectrum of ANi1 (□) and ANi2 (●; both 5 μM) in the presence of Ni^{2+} ions (1 mM). These data were obtained in HEPES buffer. The excitation wavelengths for one- and two-photon processes were 375 and 750 nm, respectively. The data for BODIPY (▲) were taken from reference [21].

The titration curves for ANi1 and ANi2 fitted well with a 1:1 binding model, the Hill plots were linear with a slope of 1.0 (Figure 2a; see also the Supporting Information, Figure S5),[17] and the Job plot of ANi2 exhibited a maximum point at a mole fraction 0.50 (see the Supporting Information, Figure S6),[18,19] thereby indicating 1:1 complexation between the probes and Ni^{2+} ions. The dissociation constants for ANi1 calculated from the fluorescence titration curves were $K_d^{OP}=100(\pm5)$ μM and $K_d^{TP}=100(\pm8)$ μM, for the OP and TP processes, respectively.[20] Similar values were determined for ANi2 ($K_d^{OP}=88(\pm5)$ μM and $K_d^{TP}=89(\pm8)$ μM), thus indicating that the binding ability is dictated by the nature of the receptor. Moreover, the OP and TP fluorescence titration curves for the complexation of ANi1 and ANi2 with Ni^{2+} ions showed positive linear relationships up to 25 μM (1.5 ppm), thus indicating that they are suitable for the detection of Ni^{2+} ions in the order of ppm (Figure 2a; also see the Supporting Information, Figure S5).

Both ANi1 and ANi2 showed high selectivity for Ni^{2+} ions in HEPES buffer, as revealed by their unperturbed fluorescence responses in the presence of millimolar concentrations of alkali and alkaline-earth metal ions (including Na^+, K^+, Mg^{2+}, and Ca^{2+}), 100 μM of first-row transition-metal ions (Mn^{2+}, Fe^{2+}), or a Group 12 ion (Zn^{2+}). Furthermore, a dramatic increase in the fluorescence intensity was observed upon addition of 100 μM of Ni^{2+} ions to the solutions containing the probe and competing ions (Figure 3a). Cu^{2+} ions turned off the fluorescence at 100 μM, owing to its paramagnetic d^9 state, but the interference was minimal at 2 μM, thereby indicating that this probe can detect Ni^{2+} ions when the Cu^{2+}-ion concentration is less than 2 μM. Moreover, the fluorescence intensities of apo or Ni^{2+}-bound probes are pH-insensitive over the biologically relevant pH range (Figure 3b).

The TP action spectra of the Ni^{2+} complexes with ANi1 and ANi2 in buffer solutions afforded $\Phi\delta$ values of about 32 and 90 GM, respectively, at 750 nm. The three-fold-larger value of $\Phi\delta$ for ANi2-Ni^{2+} can be attributed to its larger fluorescence quantum yield, and provides an additional advantage of prolinamide as the linker. Moreover, the $\Phi\delta$ value of ANi2 is 30-fold larger than that of BODIPY (Figure 2b);[21] this finding indicates that TPM images for samples stained with ANi2 would be much brighter than those stained with a BODIPY-based probe. Furthermore, the emission spectra from the ANi2-labeled A549 cells indicated that the cytosolic Ni^{2+} ions can be selectively detected by

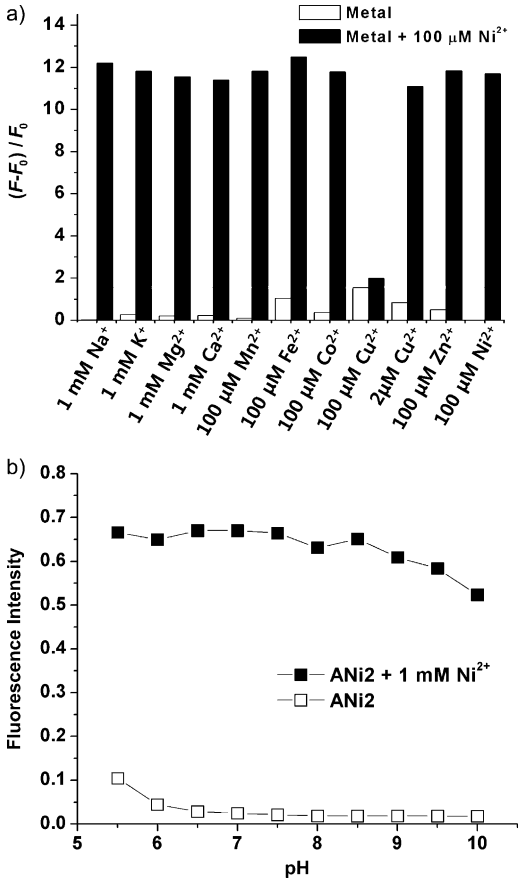

Figure 3. a) Relative fluorescence intensities of probe ANi2 (2 μM) in the presence of Na^+, K^+, Mg^{2+}, Ca^{2+} (1 mM), and other cations (100 μM; empty bars) and following the addition of Ni^{2+} ions (0.1 mM; filled bars). b) Effect of the pH value on the one-photon fluorescence intensity of ANi2 (2 μM) in the presence of 0 (□) and 1.0 mM of Ni^{2+} ions (■) in universal buffer solution. The excitation wavelength was 375 nm.

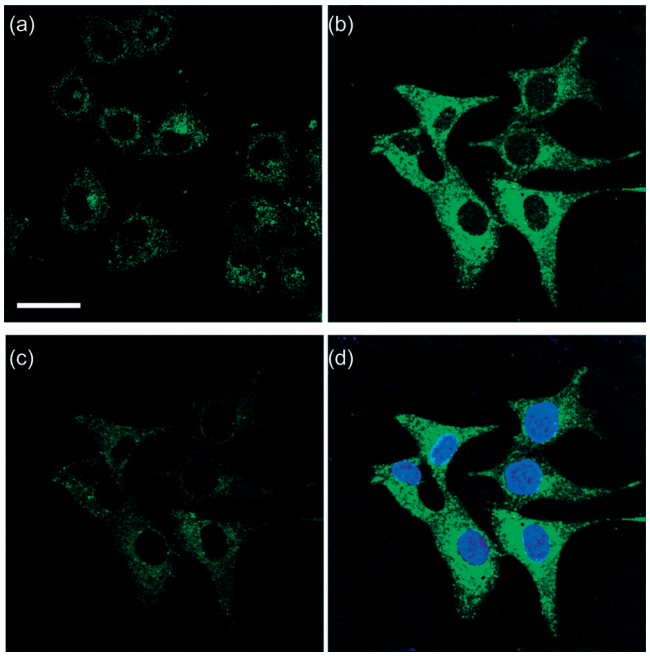

Figure 4. a–d) TPM images of A549 cells labeled with the ANi2 probe (2 μM). Cells were incubated with a 1:1 mixture of ANi2-AM (2 μM) and Pluronic F-127 for 30 min at 37 °C before (a) and after treatment with 1 mM $NiCl_2$ in the growth medium for 18 h at 37 °C (b). c) After treatment of (b) with TPEN (0.5 mM) for 1 min at 25 °C. d) $NiCl_2$ (1 mM)-supplemented cells co-stained with ANi2 and Hoescht 33342 (1 μM) to show cell viability. The TPEF was collected at 500–620 nm upon excitation at 750 nm with a fs pulse. Scale bars 30 μm. Cells shown are representative images from replicate experiments ($n=5$).

using a detection window of 500–620 nm, with minimum interference from the membrane-bound probes (see the Supporting Information, Figure S7).

Detection of Ni^{2+} ions in live cells with ANi2 by two-photon microscopy: To demonstrate the utility of this probe, we have tested the ability of ANi2 to detect Ni^{2+} ions in live cells (Figure 4). The TPM image of A549 cells labeled with ANi2 (2 μM) for 30 min at 37 °C showed weak background emission (Figure 4a), which was consistent with the efficient fluorescence quenching by PeT (see above). The TPEF intensity increased when the cells were exposed to Ni^{2+} ions (1 mM) for 18 h (Figure 4b), and decreased to the base level upon treatment with *N,N,N′,N′*-tetrakis(2-pyridyl)ethylenediamine (TPEN; 500 μM), a membrane-permeable heavy-metal ion-chelator that can effectively remove Ni^{2+} ions from the cell (Figure 4c). The cells were treated with excess Ni^{2+} ions to facilitate internalization because Ni^{2+} ions showed poor cell-permeability. The TPM image of A549 cells stained with Hoechst 33342 (Figure 4d) and the viability study using a CCK-8 kit confirmed the cell-viability (see the Supporting Information, Figure S8). Moreover, the TPEF intensity at a given spot on the ANi2-labeled A549 cells remained nearly the same after continuous irradiation of the fs pulses for 60 min,[22,23] thereby indicating its high photostability (see the Supporting Information, Figure S9). These data establish that ANi2 is capable of detecting Ni^{2+} ions in live cells with minimum interference from the pH value, other metal ions, cytotoxicity, and photostability.

Detection of Ni^{2+} ions in fish organs with ANi2 by two-photon microscopy: Next, we used probe ANi2 to investigate where Ni^{2+} ions accumulated inside fish. Thirty *Oryzias latipes* that were approximately 5 month post-hatching and fully mature with an average body weight of 0.37 g and an average length of 3.5 cm (see the Experimental Section) were acclimated in water tanks for one week. The fishes were then divided into two groups. Half of them were placed in aquaria containing 17 μM (1.0 ppm) of $NiCl_2$ and the other half in aquaria without $NiCl_2$; both groups were reared for 1 and 3 days, according to the OECD guideline for testing of chemicals in fish.[24] All of the fish survived, thereby indicating that 72 h LC_{50} value of *Oryzias latipes* is much higher than 1.0 ppm. For comparison, the 96 h LC_{50} values of other fresh-water fish, such as *Catla catla, Labeo rohita,* and *Cirrhina mrigala* were in the range 20–45 ppm.[25] The fish were killed, and their kidneys, hearts, gills, and livers were dissected, and stained with ANi2-AM. Because

it takes a long time to stain the organs, during which time they may become deformed, excess amounts (20 μM) of ANi2-AM were used to facilitate staining. The TPM images of the ANi2-labeled organs obtained at different depths showed that the Ni^{2+} ions were almost evenly distributed along the *z* direction (see the Supporting Information, Figure S10). Moreover, the images obtained at higher magnification clearly revealed the sites of Ni^{2+}-ion accumulation, that is: the glomerulus of the kidney, blood vessels in the heart, hepatocyte in the liver, and gill filaments in the gill (Figure 5). These results demonstrate that ANi2 is capable of tracing the sites of Ni^{2+}-ion accumulation in fresh fish.

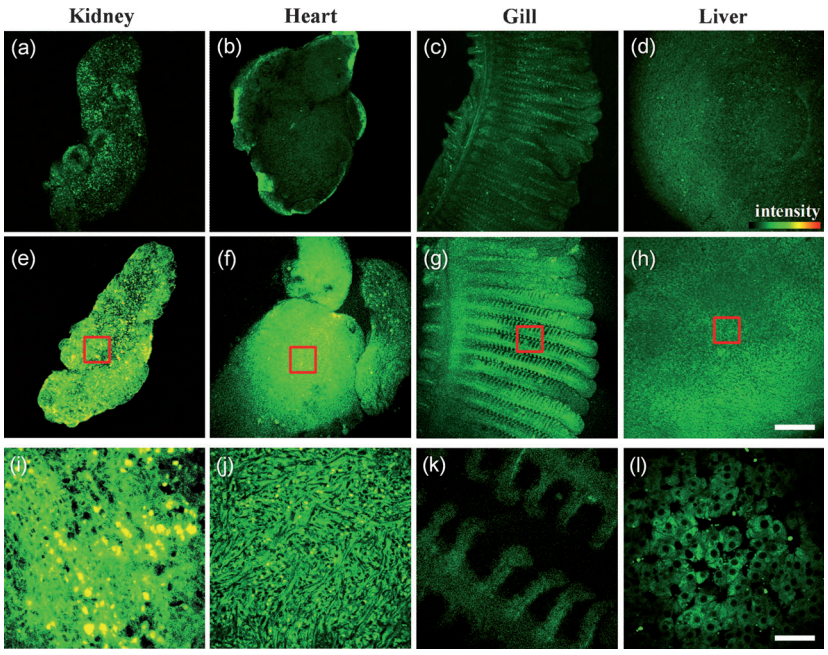

Figure 5. a–h) TPM images of the kidney, heart, gill, and liver of *Oryzias latipes* reared in aquaria containing 0 (a–d) and 17 μM (1.0 ppm) $NiCl_2$ (e–h). The images were obtained at 100 μm depth by 10× magnification. i–l) The regions indicated by the red boxes in (e–h) are magnified by 100×. All organs were stained with a 1:1 mixture of ANi2-AM (20 μM) and Pluronic F-127 for 30 min at 37 °C and the TPM images were obtained by collecting the TPEF over the range 500–620 nm upon excitation at 750 nm with fs pulses. Scale bars 300 (a–h) and 30 μm (i–l).

Furthermore, we applied probe ANi2 to estimate the Ni^{2+}-ion concentration in each organ using TPM. For this purpose, the average TPEF intensity was determined from 40 TPM images (10 images in the *xy* plane along the *z* direction of 10 organ samples). The TPEF intensity increased with exposure time and decreased with the organ in the order: kidney > heart > gill ≥ liver (Figure 6). This result indicates that Ni^{2+} ions accumulated in the same order. A similar result was reported for Hg^{2+}-ion distribution in fish.[26] We also measured the Ni^{2+}-ion content in each organ by ICP-MS. For this experiment, we used 5 organ samples because the fish organs were so small that it was difficult to gather sufficient quantity for the analysis. The result showed a linear relationship between the TPEF intensity and the ICP-MS result over a range of 1–50 ppm. Therefore, ANi2 is clearly capable of detecting Ni^{2+} ions over a wide range of concentration in edible fish.

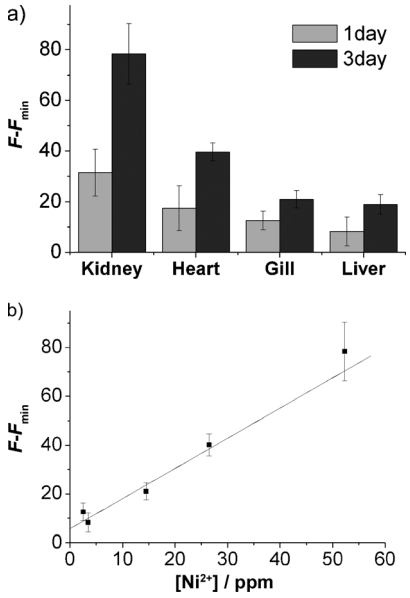

Figure 6. a) Relative TPEF intensities in the kidney, heart, gill, and liver of *Oryzias latipes* after exposure to Ni^{2+} ions (1.0 ppm) for 1 or 3 days. The organs were incubated with a 1:1 mixture of ANi2-AM (20 μM) and Pluronic F-127 for 30 min at 37 °C and the TPEF was collected over the range 500–620 nm upon excitation with fs pulses at 750 nm. The column heights and error bars represent the average and standard deviation of the TPEF intensities from 96 TPM images, respectively. b) Plot of $F-F_{min}$ against the $[Ni^{2+}]$ for: liver (1 day), gill (1 day), liver (3 days), heart (3 days), and kidney (3 days).

Conclusion

We have developed a TP probe (ANi2) that shows 26-fold TPEF enhancement in response to Ni^{2+} ions, with a dissociation constant (K_d^{TP}) of 89(±8) μM, and can selectively detect Ni^{2+} ions in live cells and fish organs at depths of 80–150 μm by TPM without interference from other metal ions or membrane-bound probes. Unlike other currently available probes, this probe can not only visualize the site of Ni^{2+}-ion accumulation, but also can estimate the trace amount of $[Ni^{2+}]$ in fresh fish organs by TPM. We found that the use of prolinamide as the linker increased the fluorescence-en-

hancement factor and TP action cross-section by a factor of 3–5. This result provides a useful guideline for the design of efficient TP probes.

Experimental Section

Synthesis: 6-Acyl-2-[*N*-methyl-*N*-(carboxymethyl)amino]naphthalene[27] (acedane, **A**) and 2,2′-(4-nitrophenylazanediyl)bis(ethane-2,1-diyl)bis(4-methylbenzenesulfonate)[28] (**1**) were prepared according to literature methods. The synthesis of other compounds is described below.

Synthesis of compound 2: A solution of compound **1** (3.0 g, 5.6 mmol) in anhydrous DMF (35 mL) was added dropwise over 1 h to a mixture of methyl thioglycolate (1.1 mL, 12 mmol) and Cs_2CO_3 (4.0 g, 12 mmol) in anhydrous DMF (20 mL) at room temperature. The reaction mixture was stirred overnight at 60 °C. The reaction mixture was filtered and the salts were washed with DMF. The resulting solution was extracted with EtOAc and washed three times with water and brine. The organic phase was dried over Na_2SO_4, filtered, and evaporated. The product was purified by column chromatography on silica gel (*n*-hexane/EtOAc, 2:1) as the eluent to obtain a yellow oil. Yield 1.7 g (77%); ^{1}H NMR (300 MHz, $CDCl_3$): δ = 8.15 (2H, d, J = 9.3 Hz), 6.70 (2H, d, J = 9.3 Hz), 3.76 (6H, s), 3.70 (4H, t, J = 7.7 Hz), 3.30 (4H, s), 2.88 ppm (4H, t, J = 7.7 Hz); IR (NaCl): $\tilde{\nu}$ = 1747, 1606, 1344 cm^{-1}; HRMS (EI): m/z calcd for $[M+H]^+$ 403.0998; found: 403.0998.

Synthesis of compound 3: A mixture of compound **2** (1.7 g, 4.3 mmol) and $SnCl_2$ (12 g, 52 mmol) in MeCN/EtOH (1/1, v/v, 150 mL) was heated to reflux for 12 h. The mixture was concentrated and a small amount of NaOH (aq) was added until a white precipitate had formed. The precipitate was filtered and the product was extracted with CH_2Cl_2, dried over $MgSO_4$, and evaporated to obtain dark brown oil. Yield 1.4 g (85%); ^{1}H NMR (300 MHz, $CDCl_3$): δ = 6.75 (2H, d, J = 8.4 Hz), 6.65 (2H, d, J = 8.4 Hz), 3.73 (6H, s), 3.45 (4H, t, J = 7.8 Hz), 3.26 (4H, s), 2.77 ppm (4H, t, J = 7.8 Hz); IR (NaCl): $\tilde{\nu}$ = 3439, 3358, 1732 cm^{-1}; HRMS (EI): m/z calcd for $[M]^+$ 372.1178; found: 372.1174.

Synthesis of B: A mixture of 2-acetyl-6-hydoxynaphthalene (1.5 g, 8.1 mmol), L-proline (4.5 g, 39 mmol), $Na_2S_2O_5$ (3.1 g, 16 mmol), NaOH (1.6 g, 39 mmol), and H_2O (25 mL) was stirred in a steel-bomb reactor at 140 °C for 96 h. The mixture was cooled to room temperature, washed with water, and acidified with dilute HCl to pH 2–3 in an ice bath. The precipitate was collected by filtration, washed with water, and purified by column chromatography on silica gel ($CHCl_3$/MeOH, 4:1). Yield 1.7 g (76%); ^{1}H NMR (300 MHz, $CDCl_3$): δ = 8.39 (1H, d, J = 1.8 Hz), 7.86 (1H, dd, J = 8.4, 1.8 Hz), 7.85 (1H, d, J = 8.4 Hz), 7.62 (1H, d, J = 9.0 Hz), 7.05 (1H, dd, J = 9.0, 2.4 Hz), 6.78 (1H, d, J = 2.4 Hz), 4.37 (1H, dd, J = 8.4, 2.1 Hz), 3.72 (1H, m), 3.53 (1H, m), 2.30–2.45 (1H, m), 2.00–2.26 ppm (3H, m); IR (KBr): $\tilde{\nu}$ = 3427, 1654, 1618 cm^{-1}; HRMS (EI): m/z calcd for $[M+H]^+$ 284.1287; found: 284.1285.

Synthesis of ANi1-Me: A mixture of compound **A** (0.37 g, 1.5 mmol), DCC (0.38 g, 1.8 mmol), and HOBt (0.23 g, 1.7 mmol) in CH_2Cl_2 (15 mL) was stirred at room temperature for 30 min. To this mixture, compound **3** (0.63 g, 1.7 mmol) in CH_2Cl_2 (5 mL) were added and stirred overnight under an Ar atmosphere. The resulting mixture was filtered and the filtrate was extracted with saturated $NaHCO_3$ (aq), dried over Na_2SO_4, filtered, and concentrated under reduced pressure. The crude product was purified by column chromatography on silica gel ($CHCl_3$/MeOH, 40:1). Yield 0.69 g (74%); m.p.: 180 °C; ^{1}H NMR (300 MHz, $CDCl_3$): δ = 8.36 (1H, d, J = 1.8 Hz), 8.02 (1H, s), 8.00 (1H, dd, J = 8.7, 1.8 Hz), 7.90 (1H, d, J = 9.3 Hz), 7.73 (1H, d, J = 8.7 Hz), 7.34 (2H, d, J = 9.0 Hz), 7.20 (1H, dd, J = 9.3, 2.4 Hz), 7.07 (1H, d, J = 2.4 Hz), 6.66 (2H, d, J = 9.0 Hz), 4.12 (2H, s), 3.73 (6H, s), 3.54 (4H, t, J = 7.2 Hz), 3.25 (4H, s), 3.25 (3H, s), 2.80 (4H, t, J = 7.2 Hz), 2.69 ppm (3H, s); IR (KBr): $\tilde{\nu}$ = 1626, 1578, 1535 cm^{-1}; HRMS (EI): m/z calcd for $[M+H]^+$ 611.2157; found: 611.2153.

Synthesis of ANi2-Me: Synthesized according to the same procedure as described for ANi1-Me, except that compound **B** (0.30 g, 1.1 mmol) was used in place of compound **A**. The crude product was purified by column chromatography on silica gel (*n*-hexane/EtOAc, 1:1) as the eluent. Yield 0.38 g (56%); m.p. 205 °C; ^{1}H NMR (400 MHz, $CDCl_3$): δ = 8.20 (1H, d, J = 1.6 Hz), 8.12 (1H, s), 7.82 (1H, dd, J = 8.8, 1.6), 7.72 (1H, d, J = 9.2 Hz), 7.54 (1H, d, J = 8.8.), 7.25 (2H, d, J = 8.8), 6.98 (1H, dd, J = 9.2, 2.4), 6.82 (1H, d, J = 2.4), 6.53 (2H, d, J = 8.8), 4.19 (1H, m), 3.79 (1H, m), 3.62(6H, s), 3.41 (4H, t, J = 7.6), 3.32 (1H, m), 3.14 (4H, s), 2.68 (4H, t, J = 7.6), 2.54 (3H, s), 2.31 (2H, m), 2.04 ppm (2H, m); ^{13}C NMR (100 MHz, $CDCl_3$): δ = 197.6, 171.1, 170.6, 147.0, 143.8, 137.1, 131.3, 131.0, 130.1, 127.0, 126.3, 125.9, 124.6, 122.2, 116.4, 112.2, 106.8, 64.6, 52.3, 50.8, 49.7, 33.2, 31.5, 29.5, 26.3, 24.0 ppm; IR (KBr): $\tilde{\nu}$ = 1736, 1624, 1522 cm^{-1}; HRMS (EI): m/z calculated for $[M+H]^+$ 638.2359; found: 638.2357.

Synthesis of ANi1: A solution of KOH in EtOH (1.0 M, 4.1 mL) was added to ANi1-Me (0.50 g, 0.82 mmol) in EtOH/CH_2Cl_2 (8:2, 10 mL) and stirred for 2 h. The solution was evaporated until the volume had been reduced by half. To this solution, dilute HCl (aq) was added slowly to pH 3–4. The product precipitated as yellow–brown solid. The product was collected, washed with distilled water, and purified by crystallization from MeOH. Yield 0.21 g (44%); m.p.: 101 °C; IR (KBr): $\tilde{\nu}$ = 3423, 1716, 1618, 1516 cm^{-1}; ^{1}H NMR (400 MHz, $CDCl_3$/[D$_4$]MeOH 9:1): δ = 8.32 (1H, d, J = 1.8 Hz), 7.93 (1H, dd, J = 8.8, 1.8 Hz), 7.85 (1H, d, J = 8.8 Hz), 7.68 (1H, d, J = 9.0 Hz), 7.26 (2H, d, J = 8.0 Hz), 7.14 (1H, dd, J = 9.0, 2.7 Hz), 7.01 (1H, d, J = 2.7 Hz), 6.60 (2H, d, J = 8.0 Hz), 4.09 (2H, s), 3.50 (4H, t, J = 7.5 Hz), 3.22 (7H, s), 2.75 (4H, t, J = 7.5 Hz), 2.65 ppm (3H, s); ^{13}C NMR (100 MHz, $CDCl_3$/[D$_4$]MeOH 9:1): δ = 198.56, 172.92, 168.21, 148.99, 144.17, 137.18, 131.51, 131.16, 130.29, 126.63, 126.30, 126.08, 124.64, 122.43, 116.23, 112.22, 106.94, 58.42, 50.75, 39.90, 33.61, 29.30, 26.28 ppm; HRMS (EI): m/z calculated for $[M+H]+$ 584.1889; found: 584.1885.

Synthesis of ANi2: Synthesized by the same procedure as described for ANi1 by using KOH in EtOH (1.0 M, 2.1 mL) and ANi2-Me (0.27 g, 0.42 mmol) in EtOH/EtOAc (4/1, v/v, 5 mL). Yield, 0.15 g (58%); m.p.: 113 °C; IR (KBr): $\tilde{\nu}$ = 3431, 1714, 1616, 1522 cm^{-1}; ^{1}H NMR (400 MHz, $CDCl_3$/[D$_4$]MeOH 9:1): δ = 8.32 (1H, d, J = 1.6 Hz), 8.17 (1H, s), 7.89 (1H, dd, J = 9.2, 1.6 Hz), 7.84 (1H, d, J = 9.2 Hz), 7.65 (1H, d, J = 9.2 Hz), 7.21 (2H, d, J = 8.8 Hz), 7.05 (1H, dd, J = 9.2, 2.4 Hz), 6.90 (1H, d, J = 2.4 Hz), 6.57 (2H, d, J = 8.8 Hz), 4.24 (1H, m), 3.86 (1H, m), 3.49 (4H, t, J = 7.6 Hz), 3.43 (1H, m), 3.18 (4H, s), 2.73 (4H, t, J = 7.6, Hz), 2.64 (3H, s), 2.36 (2H, m), 2.11 ppm (2H, m); ^{13}C NMR (100 MHz, $CDCl_3$/[D$_4$]MeOH) δ = 198.50, 172.61, 171.76, 147.11, 143.90, 137.27, 131.45, 131.23, 130.44, 127.27, 126.44, 125.98, 124.63, 122.41, 116.46, 112.48, 106.83, 64.50, 51.21, 33.50, 31.48, 29.56, 29.17, 26.29, 24.03; HRMS (EI? ESI?): m/z calculated for $[M+H]^+$ 610.2046; found: 610.2045.

Synthesis of ANi2-AM: A solution of bromomethyl acetate (0.040 mL, 0.41 mmol) in anhydrous DMF (0.4 mL) was added dropwise to a solution of ANi2 (63 mg, 0.10 mmol) and DIPEA (0.16 mL, 0.92 mmol) in anhydrous DMF (2 mL). The reaction mixture was stirred overnight at room temperature and water (10 mL) was added to quench the reaction. The product was extracted with EtOAc, dried over Na_2SO_4, filtered, and concentrated in vacuo. The crude product was purified by column chromatography on silica gel (MeOH/$CHCl_3$, 1:20) to obtain a green solid. Yield, 62 mg (82%); m.p.: 54 °C; IR (KBr): $\tilde{\nu}$ = 1763, 1664, 1620, 1518 cm^{-1}; ^{1}H NMR (400 MHz, $CDCl_3$): δ = 8.24 (1H, d, J = 1.6 Hz), 8.03 (1H, S), 7.87 (1H, dd, J = 8.8, 1.6 Hz), 7.77 (1H, d, J = 8.8 Hz), 7.59 (1H, d, J = 8.8 Hz), 7.25 (2H, d, J = 9.2 Hz), 7.01 (1H, dd, J = 8.8, 2.0 Hz), 6.86 (1H, d, J = 2.0 Hz), 6.55 (2H, d, J = 9.2 Hz), 5.67 (4H, s), 4.21 (1H, m), 3.83 (1H, m), 3.44 (4H, t, J = 7.6 Hz), 3.37 (1H, m), 3.19 (4H, s), 2.71 (4H, t, J = 7.6 Hz), 2.58 (3H, s), 2.34 (2H, m), 2.07 (2H, m), 2.00 ppm (6H, s); ^{13}C NMR (100 MHz, $CDCl_3$): δ = 197.6, 171.1, 169.4, 169.0, 147.1, 143.9, 137.2, 131.5, 131.2, 130.2, 127.2, 126.4, 126.1, 124.8, 122.3, 116.5, 112.6, 107.0, 79.6, 64.8, 50.9, 49.9, 33.1, 31.6, 29.6, 26.4, 24.1, 20.6 ppm; HRMS (EI): m/z calculated for $[M+H]^+$ 754.2468; found: 754.2462.

Solubility of ANi1, ANi2, and ANi2-AM in HEPES buffer: A small amount of dye was dissolved in DMSO to prepare the stock solution (1.0×10^{-3} M). The solution was diluted to about 6.0×10^{-3}–6.0×10^{-5} M and added to a cuvette containing HEPES Buffer (3.0 mL, pH 7.1) using a

microsyringe. In all cases, the concentration of DMSO in H_2O was maintained at 0.2%.[27] The plots of fluorescence intensity against dye concentration were linear at low concentrations and showed downward curvature at higher concentrations (see the Supporting Information, Figure S1). The maximum concentration in the linear region was recorded as the solubility. The solubilities of ANi1, ANi2, and ANi2-AM in HEPES buffer were 6.0, 9.0, and 2.1 μM, respectively.

Spectroscopic measurements: Absorption spectra were recorded on a Hewlett–Packard 8453 diode array spectrophotometer and fluorescence spectra were obtained with a Amico-Bowman series 2 luminescence spectrometer with a 1 cm standard quartz cell. The fluorescence quantum yield was determined by using Coumarin 503 as the reference, according to a literature method.[29]

Computational details: Geometries of ANi1, ANi2, and [Ni] complexes (ANi1+Ni^{2+} and ANi2+Ni^{2+}) were fully optimized at the B3LYP/6–31G** level by density functional theory (DFT) calculations,[30,31] as implemented in the Gaussian 03 program.[16] The calculated HOMO and LUMO energies of ANi1, ANi2, and their fluorophore and receptor parts are summarized in the Supporting Information, Table S2. The lowest-energy conformer of ANi1 and ANi2 shows a kinked structure (see the Supporting Information, Figure S4).

Determination of apparent dissociation constants: A series of solutions containing various [Ni^{2+}] was prepared in the presence of ANi1 (2 μM) and ANi2 (2 μM) in HEPES buffer (20 mM) and they were adjusted to pH 7.1. The apparent dissociation constant (K_d) was determined using the following equation: $F-F_{min}=[Ni^{2+}](F_{max}-F_{min})/(K_d+[Ni^{2+}])$, where F is the observed fluorescence, F_{max} is the fluorescence for the Ni^{2+}-ANi1 and Ni^{2+}-ANi2 complexes, and F_{min} is the fluorescence for free ANi1 and ANi2. The K_d value that best fit the titration curve (Figure 2a; also see the Supporting Information, S5) was calculated by using the Excel program as reported.[20] To determine the K_d^{TP} value for the two-photon process, the TPEF intensity values were recorded in the range 500–620 nm with a DM IRE2 Microscope (Leica) excited by a mode-locked titanium-sapphire laser source (Coherent Chameleon, 90 MHz, 200 fs) set at wavelength 750 nm and output power 1230 mW, which corresponded to approximately 10 mW average power in the focal plane.

Measurement of two-photon cross-section: The two-photon cross-section (δ) was determined by using femtosecond (fs) fluorescence measurement technique as described.[32] ANi1 and ANi2 were dissolved in 20 mM HEPES buffer (pH 7.1) at concentrations of 5.0×10^{-6} M and the two-photon-induced fluorescence intensity was measured in the range 720–900 nm by using rhodamine 6G as the reference, whose two-photon property has been well-characterized in the literature.[33] The intensities of the two-photon-induced fluorescence spectra of the reference and the sample were determined at the same excitation wavelength. The TPA cross-section was calculated by using $\delta=\delta_r(S_s\Phi_r\phi_r c_r)/(S_r\Phi_s\phi_s c_s)$: where the subscripts s and r stand for the sample and reference molecules, respectively. The intensity of the signal collected by a CCD detector was denoted as S, Φ is the fluorescence quantum yield, ϕ is the overall fluorescence-collection efficiency of the experimental apparatus. The number density of the molecules in solution was denoted as c. δ_r is the TPA cross-section of the reference molecule.

Cell culture and imaging: A549 human lung carcinoma cells were cultured in RPMI 1640 (WelGene) supplemented with heat-inactivated 10% FBS (WelGene), penicillin (100 units mL^{-1}), and streptomycin (100 ug mL^{-1}). All of the cells were maintained in a humidified atmosphere of CO_2/air (5:95, v/v) at 37°C. Two days before imaging, the cells were passed and plated on glass-bottomed dishes (MatTek). For labeling, the growth medium was removed and replaced with RPMI1640 without FBS. The cells were incubated with 2 μM ANi2-AM and Pluronic F-127 for 30 min at 37°C and were washed three times with RPMI1640 without FBS. The cells were washed three times with phosphate buffered saline (PBS; Gibco) and then imaged.

Two-photon fluorescence microscopy: Two-photon fluorescence microscopy images of ANi2-labeled cells and tissues were obtained with spectral confocal and multiphoton microscopes (Leica TCS SP2) with a 100× (NA = 1.30 OIL) and a 10× (NA = 0.30 DRY) objective lens, respectively. The two-photon fluorescence microscopy images were obtained with a DM IRE2 Microscope (Leica) by exciting the probes with a mode-locked titanium–sapphire laser source (Coherent Chameleon, 90 MHz, 200 fs) set at wavelength 750 nm and output power 1230 mW, which corresponded to approximately 10 mW average power in the focal plane. To obtain images in the ranges 360–460 nm and 500–620 nm, internal PMTs were used to collect the signals in an 8 bit unsigned 512×512 pixels at 400 Hz scan speed.

Detection window: The pseudocolored TPM images of cultured A549 cells treated with ANi2-AM (2 μM) showed intense spots and homogeneous domains with two-photon-emission maxima at 459 (blue) and 486 nm (red; see the Supporting Information, Figure S7). The TPEF spectrum of the intense spots was asymmetrical and could be fitted to two Gaussian functions with emission maxima at 449 (green) and 480 nm (orange), whereas the TPEF spectrum of the homogeneous domain could be fitted to a single Gaussian function (pink) with an emission maximum at 485 nm. The longer-wavelength band of the dissected Gaussian function (orange) is similar to the band of the single Gaussian function (pink). This result suggests that the probe is located in two regions of different polarity: a more-polar region that is likely to be cytosol and a less-polar region that is likely to be membrane-associated. Moreover, the shorter-wavelength band (green) in the dissected Gaussian function decreases to the baseline at wavelengths <500 nm. Therefore, cytosolic ANi2 can be selectively detected by using the detection window of 500–620 nm, with minimum interference from the membrane-bound probes.

Cell viability: To confirm that the probe couldn't affect the viability of A549 cells under our incubation conditions, we used CCK-8 kit (Cell Counting Kit-8, Dojindo, Japan) according to the manufacturers' procedure. The results are shown in the Supporting Information, Figure S8.

Photostability: The photostability of ANi2 was determined by monitoring the change in TPEF intensity with time for the ANi2-labeled A549 cells chosen without bias, as reported previously.[22,23] The TPEF intensity remained nearly the same for 1 h, thus indicating high photostability.

Preparation and staining of *Oryzias latipes* organs: *Oryzias latipes* were acquired from the Korea National Institute of Environmental Research. For this experiment, 30 *Oryzias laptipes*, approximately 5 months post-hatching and fully matured, with an average body weight of 0.37 g and an average length of about 3.5 cm long, were acclimated in water tanks for 1 week. Growth conditions followed guidelines recommended by the international toxicity test protocol (OECD 1992; http://www.env.go.jp/chemi/kagaku/). The fishes were then divided into two groups. Half of them were placed in aquaria containing 1.0 ppm of Ni^{2+} ions and the other half in aquaria without Ni^{2+} ions; both groups were reared for 1 and 3 days, according to the OECD guideline for the testing of chemicals in fish.[24] The fish were killed after being stunned by ice-cold artificial cerebrospinal fluid (ACSF; 124 mM NaCl, 3 mM KCl, 26 mM $NaHCO_3$, 1.25 mM NaH_2PO_4, 10 mM D-glucose, 2.4 mM $CaCl_2$, and 1.3 mM $MgSO_4$), and their kidneys, gills, livers, and hearts were dissected. The organs were incubated with ANi2-AM (20 μM) and Pluronic F-127 in ACSF bubbled with O_2/CO_2 (95:5) for 30 min at 37°C, washed three times with ACSF, and transferred to glass-bottomed dishes (MatTek) for imaging by a spectral confocal multiphoton microscope.

Inductively coupled plasma mass spectrometry (ICP-MS): ICP-MS analysis of kidney samples was conducted at the Korea Basic Science Institute. Briefly, OmniTrace Ultra grade nitric acid (EM Science) was used for digestion experiments. All Teflonware was rinsed with dilute nitric acid and millipore water before use. Microwave digestions were carried out using a CEM Discover Labmate microwave synthesizer. Samples of fish organs (about 2.5 mg) were digested in nitric acid (3 mL) at 180°C with 300 W microwave irradiation for 20 min. The resulting solutions were neutralized with NaOH solution (10 M) and subjected to ICP-MS.

Acknowledgements

This work was supported by the National Research Foundation (NRF) grants funded by the Korean Government (No. 2011–0020477 and 2011–

0003815) and by the Priority Research Centers Program through the NRF funded by the Ministry of Education, Science and Technology (2011–0018396 and 2011–0022978). M.Y.K. and C.S.L. were supported by BK21 scholarships.

[1] J. R. Davis, *Corrosion: understanding the basics*; ASM International: Materials Park, Ohio, **2000**.
[2] a) R. Vinodhini, M. Narayanan, *Int. J. Exergy Int. J. Environ. Sci. Tech.* **2008**, *5*, 179–182; b) A. D. Sharma, *Indian J. Dermatol. Venereol.* **2007**, *73*, 307–312; c) E. J. Calabrese, A. T. Canada, C. Sacco, *Annu Rev Public Health* **1985**, *6*, 131.
[3] F. Bolletta, I. Costa, L. Fabbrizzi, M. Licchelli, M. Montalti, P. Pallavicini, L. Prodi, N. Zaccheroni, *J. Chem. Soc. Dalton Trans.* **1999**, *9*, 1381–1385.
[4] L. J. Jiang, Q. H. Luo, Z. L. Wang, D. J. Liu, Z. Zhang, H. W. Hu, *Polyhedron* **2001**, *20*, 2807–2812.
[5] S. C. Dodani, Q. He, C. J. Chang, *J. Am. Chem. Soc.* **2009**, *131*, 18020–18021.
[6] B. N. Giepmans, S. R. Adams, M. H. Ellisman, R. Y. Tsien, *Science* **2006**, *312*, 217–224.
[7] L. D. Lavis, R. T. Raines, *ACS Chem. Biol.* **2008**, *3*, 142–155.
[8] D. W. Domaille, E. L. Que. C. J. Chang, *Nat. Chem. Biol.* **2008**, *4*, 168–175.
[9] R. M. Williams, W. R. Zipfel, W. W. Webb, *Curr. Opin. Chem. Biol.* **2001**, *5*, 603–608.
[10] W. R. Zipfel, R. M. Williams, W. W. Webb, *Nat. Biotechnol.* **2003**, *21*, 1369–1377.
[11] F. Helmchen, W. Denk, *Nat. Methods* **2005**, *2*, 932–940.
[12] H. M. Kim, B. R. Cho, *Acc. Chem. Res.* **2009**, *42*, 863–872.
[13] H. M. Kim, B. R. Cho, *Chem. Asian J.* **2011**, *6*, 58–69.
[14] S. Sumalekshmy, C. J. Farhni, *Chem. Mater.* **2011**, *23*, 483–500.
[15] A. P. de Silva, H. Q. N. Gunaratne, T. Gunnlaugsson, A. J. M. Huxley, C. P. McCoy, J. T. Rademacher, T. E. Rice, *Chem. Rev.* **1997**, *97*, 1515–1566.
[16] Gaussian 03, Revision E.01, M. J. Frisch, G. W. Trucks, H. B. Schlegel, G. E. Scuseria, M. A. Robb, J. R. Cheeseman, Montgomery, Jr., J. A.; T. Vreven, K. N. Kudin, J. C. Burant, J. M. Millam, S. S. Iyengar, J. Tomasi, V. Barone, B. Mennucci, M. Cossi, G. Scalmani, N. Rega, G. A. Petersson, H. Nakatsuji, M. Hada, M. Ehara, K. Toyota, R. Fukuda, J. Hasegawa, M. Ishida, T. Nakajima, Y. Honda, O. Kitao, H. Nakai, M. Klene, X. Li, J. E. Knox, H. P. Hratchian, J. B. Cross, C. Adamo, J. Jaramillo, R. Gomperts, R. E. Stratmann, O. Yazyev, A. J. Austin, R. Cammi, C. Pomelli, J. W. Ochterski, P. Y. Ayala, K. Morokuma, G. A. Voth, P. Salvador, J. J. Dannenberg, V. G. Zakrzewski, S. Dapprich, A. D. Daniels, M. C. Strain, O. Farkas, D. K. Malick, A. D. Rabuck, K. Raghavachari, J. B. Foresman, J. V. Ortiz, Q. Cui, A. G. Baboul, S. Clifford, J. Cioslowski, B. B. Stefanov, G. Liu, A. Liashenko, P. Piskorz, I. Komaromi, R. L. Martin, D. J. Fox, T. Keith, M. A. Al-Laham, C. Y. Peng, A. Nanayakkara, M. Challacombe, P. M. W. Gill, B. Johnson, W. Chen, M. W. Wong, C. Gonzalez, J. A. Pople, Gaussian, Inc., Pittsburgh PA, **2003**.
[17] K. A. Connors, Binding Constant, Wiley, New York, **1987**.
[18] P. Job, *Ann. Chim.* **1928**, *9*, 113–203.
[19] C. Y. Huang, *Methods Enzymol.* **1982**, *87*, 509–525.
[20] J. R. Long, R. S. Drago, *J. Chem. Educ.* **1982**, *59*, 1037–1039.
[21] C. Xu, W. W. Webb, *J. Opt. Soc. Am. B.* **1996**, *13*, 481–490.
[22] H. M. Kim, W. J. Yang, C. H. Kim, W.-H. Park, S.-J. Jeon, B. R. Cho, *Chem. Eur. J.* **2005**, *11*, 6386–6391.
[23] H. Giloh, J. W. Sedat, *Science* **1982**, *217*, 1252–1255.
[24] OECD Guideline For Testing of Chemicals 203: *Fish*, *Acute Toxicity Test*, Adopted: July 17, **1992**.
[25] A. Javid, M. Javed, S. Abdullah, *Int. J. Inorg. Mater. Int. J. Agr. Biol.* **2007**, *9*, 139–142.
[26] C. S. Lim, D. W. Kang, Y. S. Tian, J. H. Han, H. L. Hwang, B. R. Cho, *Chem. Commun.* **2010**, *46*, 2388–2390.
[27] H. M. Kim, C. Jung, B. R. Kim, S. Y. Jung, J. H. Hong, Y. G. Ko, K. J. Lee, B. R. Cho, *Angew. Chem.* **2007**, *119*, 3530–3533; *Angew. Chem. Int. Ed.* **2007**, *46*, 3460–3463.
[28] M. W. Glenny, van de Water, G. A. Leon, J. M. Vere, A. J. Blake, C. Wilson, W. L. Driessen, J. Reedijk, M. Schroeder, *Polyhedron* **2006**, *25*, 599–612.
[29] J. N. Demas, G. A. Crosby, *J. Phys. Chem.* **1971**, *75*, 991–1024.
[30] a) W. Koch, M. C. Holthausen, *A Chemist's Guide to Density Functional Theory*, Wiley, New York, **2000**.
[31] R. G. Parr, W. Yang, *Density Functional Theory of Atoms and Molecules*; Oxford University Press: Oxford, **1989**.
[32] S. K. Lee, W. J. Yang, J. J. Choi, C. H. Kim, S. J. Jeon, B. R. Cho, *Org. Lett.* **2005**, *7*, 323–326.
[33] N. S. Makarov, M. Drobizhev, A. Rebane, *Opt. Express* **2008**, *16*, 4029–4047.

Received: October 10, 2011
Published online: January 13, 2012

